HHS Public Access

Author manuscript

J Mol Med (Berl). Author manuscript; available in PMC 2016 May 04.

Published in final edited form as:

J Mol Med (Berl). 2016 January ; 94(1): 37–49. doi:10.1007/s00109-015-1356-1.

Angiotensin-converting enzyme 2 inhibits high-mobility group box 1 and attenuates cardiac dysfunction post-myocardial ischemia

Yan Fei Qi[1], **Juan Zhang**[1,3,4], **Lei Wang**[3], **Vinayak Shenoy**[3], **Eric Krause**[3], **S. Paul Oh**[2], **Carl J Pepine**[1], **Michael J Katovich**[3], and **Mohan K Raizada**[2]

Yan Fei Qi: yanfeiqi@ufl.edu; Mohan K Raizada: mraizada@ufl.edu

[1]Division of Cardiovascular Medicine, Department of Medicine, College of Medicine, University of Florida, Gainesville, FL, USA

[2]Department of Physiology and Functional Genomics, College of Medicine, University of Florida, Gainesville, FL 32610, USA

[3]Department of Pharmacodynamics, College of Pharmacy, University of Florida, Gainesville, FL, USA

[4]Department of Anesthesiology, The First Affiliated Hospital of Soochow University, Jiangsu, China

Abstract

High-mobility group box 1 (HMGB1) triggers and amplifies inflammation cascade following ischemic injury, and its elevated levels are associated with adverse clinical outcomes in patients with myocardial infarction (MI). Angiotensin-converting enzyme 2 (ACE2), a key member of vasoprotective axis of the renin-angiotensin system (RAS), regulates cardiovascular functions and exerts beneficial effects in cardiovascular disease. However, the association between HMGB1 and ACE2 has not been studied. We hypothesized that overexpression of ACE2 provides cardioprotective effects against MI via inhibiting HMGB1 and inflammation. ACE2 knock-in (KI) mice and littermate wild-type (WT) controls were subjected to either sham or coronary artery ligation surgery to induce MI. Heart function was assessed 4 weeks after surgery using echocardiography and Millar catheterization. Tissues were collected for histology and analysis of the expression of HMGB1, RAS components, and inflammatory cytokines. ACE2 in the heart of the ACE2 KI mice was 58-fold higher than WT controls. ACE2-MI mice exhibited a remarkable preservation of cardiac function and reduction of infarct size in comparison to WT-MI mice. Notably, ACE2 overexpression significantly reduced the MI-induced increase in apoptosis, macrophage infiltration, and HMGB1 and pro-inflammatory cytokine expression (TNF-α and IL-6). Moreover, in an in vitro study, ACE2 activation prevented the hypoxia-induced cell death and upregulation of HMGB1 in adult cardiomyocytes. This protective effect is correlated with

Correspondence to: Yan Fei Qi, yanfeiqi@ufl.edu; Mohan K Raizada, mraizada@ufl.edu.

Yan Fei Qi and Juan Zhang contributed equally to this work.

Compliance with ethical standards

Disclosures None.

downregulation of HMGB1 and downstream pro-inflammatory cascades, which could be useful for the development of novel treatment for ischemic heart disease.

Keywords

ACE2; Myocardial infarction; HMGB1; Inflammation

Introduction

Despite the significant advances in pharmacological and interventional therapies, ischemic heart disease remains a leading cause of death in the USA with an estimated 0.8 million Americans experiencing a new myocardial infarction (MI) each year [1]. The renin-angiotensin system (RAS), a hormonal system, plays a critical role in the pathophysiology of ischemic heart disease [2]. Increasing evidence suggests that angiotensin-converting enzyme 2 (ACE2), a key component of the RAS, could be a therapeutic target for ischemic heart disease. ACE2 knockout animals become more susceptible to cardiac problems than wild-type controls [3, 4]. Loss of ACE2 increased mortality and adverse ventricular remodeling after MI [5]. We and others have demonstrated that overexpression of ACE2 by viral vectors protects cardiac function from MI [6, 7]. Furthermore, activation of endogenous ACE2 by a small molecule offers cardiac protection against ischemia [8]. However, the intrinsic mechanisms that contribute to the cardioprotective effects of ACE2 in ischemic heart disease are yet to be elucidated.

A series of inflammatory responses occur in the necrotic tissues following a MI. Although this post-infarct inflammation is essential for the healing process, excessive inflammation leads to poor prognosis and heart failure [9]. An elevated inflammatory status is a predictor of adverse outcome in patients with cardiovascular diseases [10]. Emerging evidence indicates that ACE2 possesses an anti-inflammatory effect. ACE2 and its product, angiotensin-(1–7) [Ang-(1–7)], counteract the pro-inflammatory action of the classic vasodeleterious axis of the RAS (ACE/AngII axis) in conditions such as heart failure, pulmonary hypertension, and diabetes [11, 12]. We and others have shown that increasing ACE2 levels and activity or overexpressing Ang-(1–7) reduces inflammation in the ischemic myocardium [8, 13–15].

Both ACE inhibitors and angiotensin II receptor blockers have been found to upregulate ACE2 levels [16]. Recent studies also suggest that treatment of hypertension in patients with autosomal dominant polycystic kidney diseases with ACE inhibitors and angiotensin II receptor blockers leads to a decrease in serum level of high-mobility group box 1 (HMGB1) [17, 18]. HMGB1, a nonhistone DNA binding protein which is involved in stabilization of DNA and regulation of gene transcription, is actively released by necrotic cardiomyocytes in response to ischemia and acts to recruit inflammatory cells [19]. Inflammatory cells such as monocytes, macrophages, and dendritic cells secrete HMGB1 and, hence, further enhance the inflammatory reaction [19]. As a damage-associated molecular pattern (DAMP) molecule, HMGB1 signals through the receptor for advanced glycation end-products (RAGE), Toll-like receptor 2 (TLR2), and Toll-like receptor 4 (TLR4), subsequently

stimulating inflammatory cells to release pro-inflammatory cytokines including tumor necrosis factor-α (TNF-α), interleukin-1 (IL-1), and IL-6 [20, 21]. Additionally, HMGB1 initiates inflammatory cascades which contribute to cardiac dysfunction and remodeling [9]. Therefore, we hypothesized that overexpression of ACE2 would decrease levels of HMGB1 in the ischemic myocardium which in turn would reduce inflammatory status and prevent MI-induced cardiac dysfunction. ACE2 knock-in (KI) mice were used to investigate this hypothesis.

Methods and materials

Animals and ethics statements

All procedures involving experimental animals were approved by the Institutional Animal Care and Use Committee at the University of Florida and complied with National Institutes of Health guidelines. Animals were maintained under a 12:12 h light/dark cycle at 25±1 °C, with unrestricted access to standard food and water.

ACE2 transgenic mice

ROSA26$^{Ace2/+}$ mice (created by Dr. S. Paul Oh, University of Florida) expressing the FLAG-tagged mouse ACE2 gene under the control of the endogenous *ROSA26* promoter on one allele were generated by using *Cre-Lox* technology. Briefly, a gene cassette containing FLAG-tagged mouse ACE2 proceeded by a *loxP*-flanked Neo-STOP cassette was inserted after the *ROSA26* locus to generate *ROSA26*$^{Floxed\ Neo\text{-}STOP,Ace2/+}$ mice. After bred to germline *Cre* deleter mice (β-actin-Cre or Alk1Cre), offspring of these *ROSA26*$^{Floxed\ Neo\text{-}STOP,Ace2/+}$ mice had the *floxed Neo-STOP* cassette deleted, namely the *ROSA26*$^{Ace2/+\beta\text{-}actin\text{-}Cre/+}$ mice. Through a series of breeding steps, β-actin-Cre was then removed to generate R*OSA26*$^{Ace2/+}$ mice. These *ROSA26*$^{Ace2/+}$ mice were then inbred to generate *ROSA26*$^{Ace2/Ace2}$ and wild-type littermate control mice, which were maintained on a 129/B6 mixed background. Based on the generation technology, these *ROSA26*$^{Ace2/Ace2}$ mice (ACE2 mice) have the ACE2 gene overexpressed all through the body.

Myocardial infarction

ACE2 transgenic mice and their littermate WT controls aged from 8 to 10 weeks were divided into four experimental groups: (1) WT-Sham (*N*=9), (2) WT-MI (*N*=10), (3) ACE2-Sham (*N*=8), and (4) ACE2-MI (*N*=9). Surgery procedures were previously described with a few modifications [22]. Mice were anesthetized with 1.5–2 % isoflurane (in 100 % oxygen) under artificial ventilation using a rodent ventilator (Kent Scientific Co., Torrington, Connecticut, USA). The adequacy of anesthesia was verified using tail pinch. The heart was exposed at the fourth intercostal space, and the left anterior descending (LAD) coronary artery was occluded permanently using a 7-0 polypropylene suture. Successful occlusion of LAD was confirmed by elevation of the ST segment of the electrocardiogram and cyanosis of anterior LV wall. Sham-operated mice underwent the same surgical procedure without the coronary ligation.

Echocardiography

Echocardiograms were performed immediately before sacrifice, 4 weeks after the MI surgery using a GE vivid7 ultrasound machine with a 12-Hz transducer (GE Healthcare, NJ, USA). Mice were anesthetized with the 1.5 % isoflurane during the assessment. M-mode echocardiography was performed in the parasternal short-axis view at the level of the papillary muscles. LV systolic function was determined by ejection fractioning: EF (%)=[(EDV−ESV)/EDV]×100. All measurements were based on the average of three consecutive cardiac cycles.

Hemodynamic measurements

Millar catheterization was performed to measure the left ventricular function 4 weeks after the MI surgery as previously described [13]. Briefly, mice were anesthetized with the 1.5 % isoflurane-oxygen mixture. By cannulating the right carotid artery, an impedance-micromanometer catheter (Millar Instruments, Houston, Texas) was introduced into the left ventricle. The catheter was interfaced to a PowerLab (ADInstruments, Colorado Springs, CO, USA) signal transduction unit. Hemodynamic measurements as well as data analyses were performed using the Chart program supplied along with the PowerLab system. The measured parameters included mean arterial pressure (MAP), heart rate (HR), left ventricular end-diastolic pressure (LVEDP), and maximal positive and negative rate of rise of the left ventricular pressure (dP/dt).

Histological analysis

Under deep anesthesia and laparotomy, the animals were perfused with 20 IU heparin-PBS. Hearts were collected and the ventricles were separated from the atria. After rinsing with 1× PBS, the ventricles were weighed and cut into three sections made perpendicular to the long axis. The basal and apex section was snap frozen in liquid nitrogen and stored at −80 °C for subsequent measurements. The middle section was used to assess the infarct size, the inflammation status, and cardiac remodeling. Briefly, the middle section was fixed in 4 % phosphate buffered formalin and embedded in paraffin for cutting into 4-μm sections. Hematoxylin/eosin (HE) staining was performed to assess the inflammation severity. An investigator blinded to treatment condition assessed the extent of inflammation as previously described using the following scale: grade 0, no inflammation; grade 1, cardiac infiltration in up to 5 % of cardiac sections area; grade 2, 6–10 %; grade 3, 11–30 %; grade 4, 31–50 %; and grade 5, 51–70%[23, 24]. Sections were also stained with Picro-Sirius Red to measure infarct size [8]. Total infarct size was calculated as a fraction of the left ventricular circumference. Cardiac remodeling was assessed by determining ventricular hypertrophy, which was calculated by normalizing the wet weights of mice heart ventricles to the tibia length (VW/TL).

HMGB1 staining and ELISA

Cross-section of the heart ventricles were used for cardiac HMGB1 detection. The middle sections of the heart were incubated overnight with HMGB1 rabbit polyclonal antibody (1:100; Abcam) at 4 °C. The next day, sections were rinsed, incubated with anti-rabbit Alexa Fluor 594 conjugated secondary antibody (1:1000, Invitrogen) at room temperature for 1 h,

and mounted with anti-fade mounting medium (Vectashield; Vector Laboratories). Images were captured using a DP71 microscope (Olympus, Japan) and analyzed using ImageJ software (U.S. National Institutes of Health). Plasma level of HMGB1 was measured using HMBG1 ELISA kit (IBL international).

Apoptosis assay-TUNEL staining

Apoptosis was determined using the terminal deoxynucleotidyl transferase–mediated dUTP nick end labeling (TUNEL) assay (TMR Red In Situ Cell Death Detection Kit) according to the manufacturer's protocol (Roche Diagnostics, Indianapolis, IN) and as previously described [5]. Nuclei were labeled with 4′,6-diamidino-2-phenylindole (DAPI). For each slide, five different fields were evaluated at high magnification (×400). The number of the apoptotic nuclei (red fluorescence) was counted using ImageJ.

Western blot

Heart tissue (from the peri-infarct region of the left ventricle) was homogenized in radioimmunoprecipitation assay buffer. Equal amounts of protein from our experimental groups were fractionated in 12%SDS-polyacrylamide gels and transferred onto nitrocellulose membranes (60 μg of total protein was loaded for detecting ACE and ACE2; 30 μg of total protein was loaded for the rest of targets). The membranes were blocked with 5 % nonfat milk solution in Tris-buffered saline (TBS) with 0.1 % Tween-20 for 1 h. Then the membranes were incubated either with primary antibody for multiple proteins including ACE2, ACE, AT_1R, AT_2R, MasR, HMGB1, and CD68 overnight at 4 °C [ACE2 goat polyclonal antibody (1:500; R&D systems), ACE rabbit polyclonal antibody (1:500; Santa Cruz Biotechnology), AT_1R rabbit polyclonal antibody (1:500; Alomone Labs), AT_2R rabbit polyclonal antibody (1:400; Alomone Labs), MasR rabbit polyclonal antibody (1:200; Alomone Labs); HMGB1 rabbit polyclonal antibody (1:1000; Abcam); CD68 mouse monoclonal antibody (1:1000; Biolegend)]. Mouse monoclonal anti-GAPDH antibody (1:2500; Sigma Aldrich) was used to confirm equal loading. The membranes were then washed three times for 5 min in TBS-T and incubated with secondary antibody conjugated with horseradish peroxidase (anti-goat, anti-rabbit, and anti-mouse IgG 1:2500; GE Healthcare) for 1 h. Finally, the membranes were subjected to a chemiluminescence detection system and exposed to a photographic film.

Real-time PCR

Tissue from vital organs (including brain, lung, heart, kidney, and liver) were collected and homogenized. Total RNA was isolated using Trizol (Invitrogen). Then 500 ng RNA was reverse transcribed using the iScript cDNA Synthesis kit (Bio-Rad, Hercules, CA, USA). ACE2, ACE, IL-6, TNF-α, and GAPDH mRNA levels were analyzed by quantitative real-time PCR using Taqman probe (Applied Biosystems). Real-time PCR was run using ABI Prism 7600 sequence detection system. All cDNA samples were assayed in triplicate. Data from each sample were normalized to GAPDH.

Plasma ACE2/ACE activity assay

Heparinized plasma was diluted at 1:10 ratio in buffer that consisted of 1 M NaCl, 75 mM Tris–HCl, and 0.5 mM $ZnCl_2$ (pH 7.4). Moreover, 10 nM ACE or ACE2 enzyme was used as positive controls. Human recombinant ACE2 (catalog 933-ZN-010) and ACE (catalog 929-ZN) were obtained from R&D Systems along with their fluorogenic substrates [ACE2 substrate—fluorogenic peptide VI (FPS VI), Mca-YVADAPK(Dnp)OH, catalog ID ES007; ACE substrate—fluorogenic peptide V (FPS V), Mca-RPPGFSAFK(Dnp)-OH, catalog ID ES005]. All reactions were performed in a total volume of 100 µl using a fluorescence plate reader (Synergy HT, Biotek, USA) at an excitation wavelength of 320 nm and emission wavelength of 405 nm as described previously [8]. All samples were read at 37 °C for 4 h immediately after the addition of fluorogenic substrate.

Plasma Ang-1–7 and Ang II ELISA

EDTA (ethylenediaminetetraacetic acid)-treated plasma was collected and passed through a C-18 column included in an extraction kit (Peninsula Laboratories, LLC) to concentrate peptide. The peptide in the plasma was then eluded into a final volume of 3 ml buffer. Subsequently, the eluent was evaporated to dryness using an automatic speedvac system (Savant, AES1010). After the concentration, the pellet was dissolved in either with EIA buffer (for Ang-1–7 ELISA) or assay buffer (for Ang-II ELISA) for subsequent assays using ELISA reagent kits (Ang-1–7 ELISA kit was obtained from Peninsula Laboratories, Inc.; Ang-II ELISA kit was obtained from Enzo Life Sciences, Inc.). All analyses were performed according to the manufacturers' instructions.

Adult rabbit ventricular myocytes: isolation and hypoxia

Hearts of New Zealand White rabbits were isolated and perfused via the aorta with warm (35 °C) and oxygenated solutions as follows: (1) Tyrode solution containing (mmol/l) 135 NaCl, 4.6 KCl, 1.8 $CaCl_2$, 1.1 $MgSO_4$, 10 glucose, and 10 HEPES, pH 7.4, for 5 min; (2) Ca^{2+}-free solution containing (mmol/l) 100 NaCl, 30 KCl, 2 $MgSO_4$, 10 glucose, 10 HEPES, 15 taurine, and 5 pyruvate, pH 7.4, for 5 min; and (3) Ca^{2+}-free solution containing collagenase (120 U/ml) and albumin (2 mg/ml) for 20 min. At the end of the perfusion, the ventricles were minced and gently shaken for 10 min in solution 3 to release single cells. A hypoxic condition was created by incubating the cells in an airtight chamber with an atmosphere of 1 % oxygen, 5 % CO_2, and 94 % nitrogen at 37 °C. Cells were suspended in Hanks/Balanced Salt Solution without calcium and magnesium and then plated into a six-well plate at 10,000 cells/well density. Cells were divided into six groups: (1) normoxia, (2) hypoxia (H), (3) H+ ACE2 activator (1 µM diminazene acetuate, DIZE), (4) H+1 µM DIZE + 1 µM C16 (a selective ACE2 blocker); (5) H+1 µMDIZE+ 1 µM PD123391 (an AT2R blocker, PD), and (6) H+1 µM DIZE+1 µM A779 (a Mas R antagonist). Four hours after exposure to hypoxia, cell viability was tested using CellQuanti-Blue™ Cell Viability Assay Kits (BioChain, Hayward, USA) as we described before [13], and the medium was collected to measure HMGB1 levels.

Statistical analysis

Data are expressed as mean±SE and were analyzed by *t* test or one-way ANOVA with Bonferroni correction for multiple comparisons. Histology scores of myocardial injury severity were compared using the Mann–Whitney *U* test between WT-MI and ACE2-MI groups. Values of $p < 0.05$ were considered statistically significant. All of the data were analyzed using GraphPad Prism 5 software (GraphPad Prism Institute Inc).

Results

Characterizations of ACE2 knock-in (KI) mice

ACE and ACE2 mRNA levels in the heart, lung, liver, kidney, spleen, and paraventricular nucleus (PVN) of the brain were quantified using real-time PCR. The PVN was selected due to its critical role in cardiovascular pathophysiology. ACE2 was significantly upregulated in the vital organs of ACE2 KI mice in comparison to WT controls (Table 1) with 5-fold, 58-fold, and 219-fold upregulation of ACE2 in the kidney, heart, and PVN, respectively. Overexpression of ACE2 did not alter the endogenous ACE levels aside from a slight elevation of ACE in the PVN. ACE2/ACE ratio was highest in the liver followed by the brain and heart. Cardiac hemodynamics and mean arterial pressure of ACE2-KI were comparable to those of WT mice (Table 2). This observation was in contrast to a previous study of Donoghue et al. who reported abnormal blood pressure and conduction anomalies including heart block and ventricular tachycardia in ACE2 transgenic mice [25].

ACE2 overexpression attenuates MI-induced left ventricle dysfunction and associated cardiac remodeling

Heart function for four groups of animals, WT-Sham, WT-MI, ACE2-Sham, and ACE2-MI mice, were measured using echocardiography and Millar catheterization. WT-MI animals showed a 59 % decrease in ejection fraction (EF), 6-fold increase in left ventricular end-systolic volume (ESV), 1.7-fold in end-diastolic volume (EDV), 52 % elevation in left ventricular end-diastolic pressure (LVEDP), 59 % decrease in dP/dt_{max}, and 39 % reduction in dP/dt_{min} as compared to WT-Sham (Table 2). ACE2 mice were protected from MI-induced damage with preserved heart function compared to WT-MI with less decrease in EF (21 % reduction for ACE2-MI vs. 59 % for WT-MI, $p<0.05$). No significant differences were observed in mean arterial pressure (MAP) and heart rate (HR) between WT and ACE2 mice for both sham and MI groups. Consistent with the echocardiographic results (Table 2 and Fig. 1a), the WT-MI mice developed ventricular hypertrophy as measured by the VW/TL ratio, which was not observed in the ACE2-MI mice (Fig. 1a). Additionally, we examined the infarcted area in the MI animals using fibrosis staining, and infarction size was quantified as the percentage of fibrotic area of the free wall of left ventricle. ACE2-MI mice demonstrated a 52 % reduction in infarct size than WT-MI mice (Fig. 1b).

ACE2 overexpression alters expression of cardiac RAS

To study the underlying mechanisms for the cardioprotective effects of ACE2 following MI, we first investigated if overexpression of ACE2 and MI modulate expression of major components of the RAS. We measured protein levels of ACE, ACE2, angiotensin II type 1

receptor (AT1R), angiotensin II type 1 receptor (AT2R), and Mas R in the free wall of left ventricles collected from WT-Sham, WT-MI, ACE2-Sham, and ACE2-MI animals. Consistent with ACE2 mRNA level in the heart (Table 1), the protein level of ACE2 in the myocardium of left ventricle free wall was dramatically increased (Fig. 2a, b) in the ACE2 animals. MI slightly increased ACE2 level for WT-MI and ACE2-MI, which was not significantly different from its corresponding control (Fig. 2a, b). At baseline, ACE protein level was not different between WT-Sham and ACE2-Sham, which was consistent with mRNA expression data. MI significantly increased ACE for WT-MI mice (Fig. 2a, c). Overexpression of ACE2 attenuated the MI-induced increase in ACE level (3-fold less in ACE2-MI than WT-MI mice; Fig. 2a, c). Cardiac AT1R levels were not influenced by overexpression of ACE2 or MI (Fig. 2a, d). However, cardiac AT2R levels were elevated by overexpression of ACE2 (2-fold increase in ACE2 mice vs. WT controls), and MI did not change the AT2R expression (Fig. 2a, e). Finally, overexpression of ACE2 decreased the Mas R expression for ACE2 mice, and MI significantly upregulated Mas R levels in WT-MI (Fig. 2a, f).

ACE2 overexpression alters plasma ACE, ACE2, Ang II, and Ang-(1–7) levels

Plasma ACE2 activity was significantly higher in ACE2-Sham mice compared with WT-Sham (Fig. 3a, b). MI further increased this activity by 31 % in ACE2-MI. In contrast, ACE2-Sham had lower ACE activity than WT-Sham, but MI increased ACE activity for both WT-MI and ACE2-MI mice (Fig. 3a, b). Furthermore, plasma Ang-(1–7) levels for ACE2-Sham and ACE2-MI were significantly higher than their respective WT controls (Fig. 3c). AngII levels tended to be less in ACE2-Sham and ACE2-MI mice than WT controls, and MI only significantly increased the plasma AngII concentration in WT-MI mice (Fig. 3d).

ACE2 overexpression prevents ischemia-induced elevation of HMGB1

HMGB1 is an important pro-inflammatory mediator in myocardial ischemia injury [26]. Thus, we measured plasma and tissue levels of HMGB1. Baseline HMGB1 levels were comparable between ACE2-Sham and WT-Sham (Fig. 4). MI resulted in 5-fold increase in plasma HMGB1 levels (Fig. 4a) and 3.8-fold increase in peri-infarct myocardium HMGB1 levels in WT-MI animals (Fig. 4b–d). These increases in both plasma and myocardium were significantly attenuated in ACE2-MI mice (Fig. 4), suggesting overexpression of ACE2 prevented the elevation of the “death signal” and possibly blocked HMBG1 downstream signaling for inflammation.

ACE2 overexpression reduces ischemia-induced infiltration of inflammatory cells and prevents apoptosis

MI resulted in significant histopathology in cardiac sections of WT-MI mice, as evidenced by loss of nuclei and of transverse striation, visible necrosis, and infiltration of inflammatory cells (Fig. 5a, b). Overexpression of ACE2 significantly decreased the histopathological score in ACE2-MI mice, indicating a reduction of inflammation (Fig. 5a, b). MI led to a 31 % increase in macrophage infiltration (CD68 as a macrophage marker) in the WT-MI, which was attenuated in ACE2-MI mice (Fig. 5c, d). The level of macrophages in the myocardium of ACE2-Sham was lower than WT-Sham further supporting that overexpression of ACE2 downregulated the inflammation in the heart following MI (Fig.5c,

d). Finally, heart sections of the WT-MI mice showed a 14-fold increase in terminal deoxynucleotidyl transferase dUTP nick end labeling (TUNEL) staining, which was prevented in ACE2-MI mice (Fig. 5e, f).

ACE2 overexpression decreases ischemia-induced increase in pro-inflammatory cytokines in heart

To further investigate the role of inflammation, protein and mRNA levels of TNF-α and IL-6 in the peri-infarct region of heart were examined. In comparison to WT-Sham, TNF-α protein was increased ~2-fold and its mRNA was increased 10-fold in the WT-MI animals (Fig. 6a, b). Increases in IL-6 protein (2-fold) and its mRNA (11-fold) were also observed in WT-MI (Fig. 6c, d). Thus, ACE2 overexpression prevented ischemia-induced elevation of TNF-α and IL-6 (Fig. 6).

ACE2 activation attenuated cell death after hypoxic treatment

Adult rabbit cardiomyocytes in culture were utilized to confirm if ACE2 effects observed in vivo are a result of its direct action on HMGB1. Hypoxia was used to mimic in vivo ischemic injury. Hypoxia resulted in a 35%decrease in cardiomyocyte viability and a 43 % increase in HMGB1 levels (Fig. 7). Treatment of cardiomyocytes with diminazene aceturate (DIZE), an ACE2 activator [13], prevented the hypoxia-induced cell death and increase in HMGB1 level. DIZE-mediated decrease in HMGB1 was blocked by C16 (ACE2 antagonist), PD123319 (AT2R antagonist), and A779 (Mas R antagonist) (Fig. 7).

Discussion

The current study offers new insights into the possible downstream signaling pathway of ACE2 and provides the first evidence, to our knowledge, of a link between ACE2 and HMGB1. HMGB1 has been implicated as a “death signal” to cells following MI [20]. In our study, we observed an increase in HMGB1 in the hearts of WT-MI animals with deteriorated heart function. This is consistent with studies of patients with MI, which demonstrate that elevated HMGB1 levels are associated with cardiac dysfunction and adverse left ventricular remodeling [21, 26–29]. Furthermore, systemic administration of recombinant HMGB1 worsened cardiac function [30]. Additionally, aHMGB1 antagonist renders protection against ischemia-reperfusion injury [31]. Thus, elevation of HMGB1 appears to be detrimental to the ischemic heart and could induce further damage after infarction. Our observation is relevant in this regard and demonstrates that the vasoprotective axis of the RAS could act via blockage of HMGB1 signaling in providing cardioprotection.

HMGB1 is synthesized in the nucleus of necrotic cardiomyocytes and secreted to serve as recruiting and stimulating signals for macrophage and neutrophils, which, in turn, are capable of secreting HMGB1 and magnifying the inflammatory cascades [21]. HMGB1 has been studied as an inflammatory mediator in a wide range of diseases, including ischemic injury in the heart, liver, and brain [21, 26–30]. Additionally, anti-HMGB1 treatment has been shown to prevent the upregulation of the cytokines TNF-α and IL-1β and the influx of macrophages [27]. In the current study, we found MI increased HMGB1 levels both in the plasma and peri-infarct area of myocardiums for the WT-MI animals; ACE2 overexpression

exerted similar effects as other anti-HMGB1 treatment and prevented the upregulation of HMGB1 in the ACE2-MI group. This effect is associated with a decreased number of infiltrated macrophages, reduced apoptosis, and downregulation of inflammatory cytokines (including TNF-α and IL-6) in the peri-infarct area. Thus, these observations suggest that HMGB1 could be a key regulation target of the anti-inflammatory pathway through which ACE2 exhibits its effects in ischemia-induced pathophysiology. Additionally, this ACE2 KI mouse model can be used to study inflammatory related diseases in other organs, such as the kidney, liver, brain, and lung.

ACE2 is an important regulatory enzyme in the RAS that converts AngII to Ang-(1–7). For the ACE2 KI mice, ACE2 was ubiquitously overexpressed in the whole body and influenced the levels of AngII and Ang-(1–7). Analysis of AngII and Ang-(1–7) revealed that overexpression of ACE2 led to an elevation of plasma Ang-(1–7) and decrease in plasma AngII with a concomitant downregulation of ACE expression and activity, shifting the RAS balances towards the vasoprotective axis of the RAS. This result is consistent with a report by our previous report [6] and a report by Zhao et al. [7], in which overexpression of ACE2 ameliorates MIinduced pathophysiology. Furthermore, Ang-(1–7) is critical in maintaining cardiovascular homeostasis. Ang-(1–7) has been shown to improve coronary artery perfusion and endothelial function [32], reduce the incidence and the duration of post-ischemia reperfusion arrhythmias [33, 34], enhance contractile function [35], and attenuate cardiac remodeling [13]. Thus, it is reasonable to speculate that Ang-(1–7) contributes to the improved heart function in the ACE2-MI mice. We also found that ACE2 was further elevated in the ACE2-MI mice, which implies that ACE2 appears to have more profound effects during pathological states like hypertension and heart failure when the RAS is active. Meanwhile, Mas R expression was downregulated in ACE2 mice, which may be due to desensitization effects induced by prolonged elevation of Ang-(1–7) in the body.

Part of ACE2-mediated beneficial effects may be attributed to AT2R. AT2R is a functional antagonist of the AT1R, contributing to vasorelaxation, natriuresis, and anti-fibrosis [36]. Currently, therapeutic potential of AT2R in cardiovascular disease is under investigation with the use of novel AT2R agonists such as compound 21 (C21). C21 improves systolic and diastolic heart functions, reduces arterial stiffness, and blunts the inflammation infiltration in the animal models of ischemic heart disease [37–39]. It has been found that crosstalk occurs between AT2R and ACE2/Ang-(1–7) axis. Sriramula et al. reported that ACE2 overexpression led to the upregulation of AT2R [40]. Stimulation of AT2R increased both ACE2 expression and activity [41, 42]. Overexpression of AT2R also upregulates the ACE2 levels in the ischemic heart [43]. The Ang-(1–7) receptor, Mas R, can functionally interact with AT2R [42], and a Mas R blocker abolished the C21-mediated protective effects in a rat model of pulmonary hypertension [44]. In this context, we observed upregulation of AT2R in the ACE2 KI animals. From our in vitro study, we found that an ACE2 selective antagonist, an AT2R antagonist, and a Mas R blocker abolished the protective actions of an ACE2 activator in the hypoxic cardiomyocytes. Taken together, these observations suggest that the ACE2-mediated beneficial effects on MI-induced cardiac pathophysiology could, in part, be attributed to the involvement of the AT2R. Further investigation would be needed to discover the mechanism of ACE2/AT2R interaction.

Reduced infarct area, along with a decrease in ventricular hypertrophy, is a noteworthy effect of overexpression of ACE2. We observed a 52 % reduction of infarct area and 28 % reduction in ventricular hypertrophy in the ACE2-MI group when compared with WT-MI. This reversal appears to be a combination effect of an upregulation of Ang-(1–7) and AT2R and a downregulation of AngII and ACE. It is well recognized that the AngII/AT1R axis induces maladaptive remodeling in the heart after injury, while the vasoprotective axis, ACE2/Ang-(1–7)/AT2R/Mas R, reverses/prevents this adverse cardiac remodeling [45]. Furthermore, we demonstrated that these ACE2 mediated cardioprotective effects in the ischemic heart are tightly associated with reduction in HMGB1 levels after MI. This is further supported by a recent study that demonstrated HMGB1 inhibition alleviates myocardial remodeling and fibrosis in diabetic cardiomyopathy [46]. Further studies are needed to further elucidate any upstream and downstream signaling pathways.

In conclusion, ACE2 overexpression prevents ischemia-induced cardiac dysfunction. The mechanism by which ACE2 produces this cardioprotective action appears to involve downregulation of HMGB1 and its associated downstream pro-inflammatory cytokines as well as modulation of the expression of other components of the RAS.

Acknowledgments

This study was supported by 5UM1HL087366-09 2 UM1 HL087366-06, R01 HL056921, HL033610, and UL1 TR000064 from the National Institutes of Health. We would like to thank Dr. Yejia Song for providing the adult cardiac myocytes and M.S. Colleen Cole-Jeffrey for editing the manuscript.

References

1. Mozaffarian D, Benjamin EJ, Go AS, Arnett DK, Blaha MJ, Cushman M, de Ferranti S, Després JP, Fullerton HJ, Howard VJ, et al. Heart disease and stroke statistics—2015 update: a report from the American Heart Association. Circulation. 2015; 131(4):e29–e322. [PubMed: 25520374]
2. Pieruzzi F, Abassi ZA, Keiser HR. Expression of renin-angiotensin system components in the heart, kidneys, and lungs of rats with experimental heart failure. Circulation. 1995; 92:3105–3112. [PubMed: 7586282]
3. Yamamoto K, Ohishi M, Katsuya T, Ito N, Ikushima M, Kaibe M, Tatara Y, Shiota A, Sugano S, Takeda S, et al. Deletion of angiotensin-converting enzyme 2 accelerates pressure overload-induced cardiac dysfunction by increasing local angiotensin II. Hypertension. 2006; 47:718–726. [PubMed: 16505206]
4. Bodiga S, Zhong JC, Wang W, Basu R, Lo J, Liu GC, Guo D, Holland SM, Scholey JW, Penninger JM, et al. Enhanced susceptibility to biomechanical stress in ACE2 null mice is prevented by loss of the p47(phox) NADPH oxidase subunit. Cardiovasc Res. 2011; 91:151–161. [PubMed: 21285291]
5. Kassiri Z, Zhong J, Guo D, Basu R, Wang X, Liu PP, Scholey JW, Penninger JM, Oudit GY. Loss of angiotensin-converting enzyme 2 accelerates maladaptive left ventricular remodeling in response to myocardial infarction. Circ Heart Fail. 2009; 2:446–455. [PubMed: 19808375]
6. Der Sarkissian S, Grobe JL, Yuan L, Narielwala DR, Walter GA, Katovich MJ, Raizada MK. Cardiac overexpression of angiotensin converting enzyme 2 protects the heart from ischemia-induced pathophysiology. Hypertension. 2008; 51:712–718. [PubMed: 18250366]
7. Zhao YX, Yin HQ, Yu QT, Qiao Y, Dai HY, Zhang MX, Zhang L, Liu YF, Wang LC, de Liu S, et al. ACE2 overexpression ameliorates left ventricular remodeling and dysfunction in a rat model of myocardial infarction. Hum Gene Ther. 2010; 21:1545–1554. [PubMed: 20507236]
8. Qi Y, Zhang J, Cole-Jeffrey CT, Shenoy V, Espejo A, Hanna M, Song C, Pepine CJ, Katovich MJ, Raizada MK. Diminazene aceturate enhances angiotensin-converting enzyme 2 activity and

attenuates ischemia-induced cardiac pathophysiology. Hypertension. 2013; 62:746–752. [PubMed: 23959549]

9. Anzai T. Post-infarction inflammation and left ventricular remodeling: a double-edged sword. Circ J. 2013; 77:580–587. [PubMed: 23358460]
10. Johnson BD, Kip KE, Marroquin OC, Ridker PM, Kelsey SF, Shaw LJ, Pepine CJ, Sharaf B, Bairey Merz CN, Sopko G, et al. Serum amyloid a as a predictor of coronary artery disease and cardiovascular outcome in women: the National Heart, Lung, and Blood Institute-Sponsored Women's Ischemia Syndrome Evaluation (WISE). Circulation. 2004; 109:726–732. [PubMed: 14970107]
11. Gaddam RR, Chambers S, Bhatia M. ACE and ACE2 in inflammation: a tale of two enzymes. Inflamm Allergy Drug Targets. 2014; 13:224–234. [PubMed: 25019157]
12. Ferrario CM, Jessup J, Chappell MC, Averill DB, Brosnihan KB, Tallant EA, Diz DI, Gallagher PE. Effect of angiotensin-converting enzyme inhibition and angiotensin II receptor blockers on cardiac angiotensin-converting enzyme 2. Circulation. 2005; 111:2605–2610. [PubMed: 15897343]
13. Qi Y, Shenoy V, Wong F, Li H, Afzal A, Mocco J, Sumners C, Raizada MK, Katovich MJ. Lentivirus-mediated overexpression of angiotensin-(1–7) attenuated ischaemia-induced cardiac pathophysiology. Exp Physiol. 2011; 96:863–874. [PubMed: 21685447]
14. Xue T, Wei N, Xin Z, Qingyu X. Angiotensin-converting enzyme-2 overexpression attenuates inflammation in rat model of chronic obstructive pulmonary disease. Inhal Toxicol. 2014; 26:14–22. [PubMed: 24417403]
15. Simões e Silva AC, Silveira KD, Ferreira AJ, Teixeira MM. ACE2, angiotensin-(1–7) and Mas receptor axis in inflammation and fibrosis. Br J Pharmacol. 2013; 169:477–492. [PubMed: 23488800]
16. Ishiyama Y, Gallagher PE, Averill DB, Tallant EA, Brosnihan KB, Ferrario CM. Upregulation of angiotensin-converting enzyme-2 after myocardial infarction by blockade of angiotensin II receptors. Hypertension. 2004; 43:970–976. [PubMed: 15007027]
17. Kikuchi K, Tancharoen S, Ito T, Morimoto-Yamashita Y, Miura N, Kawahara K, Maruyama I, Murai Y, Tanaka E. Potential of the angiotensin receptor blockers (ARBs) telmisartan, irbesartan, and candesartan for inhibiting the HMGB1/RAGE axis in prevention and acute treatment of stroke. Int J Mol Sci. 2013; 14:18899–18924. [PubMed: 24065095]
18. Nakamura T, Sato E, Fujiwara N, Kawagoe Y, Yamada S, Ueda Y, Koide H. Changes in urinary albumin excretion, inflammatory and oxidative stress markers in ADPKD patients with hypertension. Am J Med Sci. 2012; 343:46–51. [PubMed: 21760473]
19. Andrassy M, Volz HC, Igwe JC, Funke B, Eichberger SN, Kaya Z, Buss S, Autschbach F, Pleger ST, Lukic IK, et al. High-mobility group box-1 in ischemia-reperfusion injury of the heart. Circulation. 2008; 117:3216–3226. [PubMed: 18574060]
20. Klune JR, Dhupar R, Cardinal J, Billiar TR, Tsung A. HMGB1: endogenous danger signaling. Mol Med. 2008; 14:476–484. [PubMed: 18431461]
21. de Haan JJ, Smeets MB, Pasterkamp G, Arslan F. Danger signals in the initiation of the inflammatory response after myocardial infarction. Mediators Inflamm. 2013; 2013:206039. [PubMed: 24363498]
22. Zhang J, Song J, Xu J, Chen X, Yin P, Lv X, Wang X. ERK1/2-Egr-1 signaling pathway-mediated protective effects of electroacupuncture in a mouse model of myocardial ischemia-reperfusion. Evid Based Complement Alternat Med. 2014; 2014:253075. [PubMed: 24883066]
23. Theiss HD, Gross L, Vallaster M, David R, Brunner S, Brenner C, Nathan P, Assmann G, Mueller-Hoecker J, Vogeser M, et al. Antidiabetic gliptins in combination with G-CSF enhances myocardial function and survival after acute myocardial infarction. Int J Cardiol. 2013; 168:3359–3369. [PubMed: 23669105]
24. Goser S, Andrassy M, Buss SJ, Leuschner F, Volz CH, Ottl R, Zittrich S, Blaudeck N, Hardt SE, Pfitzer G, et al. Cardiac troponin I but not cardiac troponin T induces severe autoimmune inflammation in the myocardium. Circulation. 2006; 114:1693–1702. [PubMed: 17015788]
25. Donoghue M, Wakimoto H, Maguire CT, Acton S, Hales P, Stagliano N, Fairchild-Huntress V, Xu J, Lorenz JN, Kadambi V, et al. Heart block, ventricular tachycardia, and sudden death in ACE2

transgenic mice with downregulated connexins. J Mol Cell Cardiol. 2003; 35:1043–1053. [PubMed: 12967627]

26. Lin Y, Chen L, Li W, Fang J. Role of high-mobility group box-1 in myocardial ischemia/reperfusion injury and the effect of ethyl pyruvate. Exp Ther Med. 2015; 9:1537–1541. [PubMed: 25780465]
27. Kohno T, Anzai T, Naito K, Miyasho T, Okamoto M, Yokota H, Yamada S, Maekawa Y, Takahashi T, Yoshikawa T, et al. Role of high-mobility group box 1 protein in post-infarction healing process and left ventricular remodelling. Cardiovasc Res. 2009; 81:565–573. [PubMed: 18984601]
28. Goldstein RS, Gallowitsch-Puerta M, Yang L, Rosas-Ballina M, Huston JM, Czura CJ, Lee DC, Ward MF, Bruchfeld AN, Wang H, et al. Elevated high-mobility group box 1 levels in patients with cerebral and myocardial ischemia. Shock. 2006; 25:571–574. [PubMed: 16721263]
29. Cirillo P, Giallauria F, Pacileo M, Petrillo G, D'Agostino M, Vigorito C, Chiariello M. Increased high mobility group box-1 protein levels are associated with impaired cardiopulmonary and echocardiographic findings after acute myocardial infarction. J Card Fail. 2009; 15:362–367. [PubMed: 19398086]
30. Hagiwara S, Iwasaka H, Uchino T, Noguchi T. High mobility group box 1 induces a negative inotropic effect on the left ventricle in an isolated rat heart model of septic shock: a pilot study. Circ J. 2008; 72:1012–1017. [PubMed: 18503231]
31. Woo YJ, Taylor MD, Cohen JE, Jayasankar V, Bish LT, Burdick J, Pirolli TJ, Berry MF, Hsu V, Grand T. Ethyl pyruvate preserves cardiac function and attenuates oxidative injury after prolonged myocardial ischemia. J Thorac Cardiovasc Surg. 2004; 127:1262–1269. [PubMed: 15115981]
32. Loot AE, Roks AJ, Henning RH, Tio RA, Suurmeijer AJ, Boomsma F, van Gilst WH. Angiotensin-(1–7) attenuates the development of heart failure after myocardial infarction in rats. Circulation. 2002; 105:1548–1550. [PubMed: 11927520]
33. Ferreira AJ, Santos RA, Almeida AP. Angiotensin-(1–7): cardioprotective effect in myocardial ischemia/reperfusion. Hypertension. 2001; 38:665–668. [PubMed: 11566952]
34. De Mello WC. Angiotensin (1–7) re-establishes impulse conduction in cardiac muscle during ischaemia-reperfusion. The role of the sodium pump. J Renin Angiotensin Aldosterone Syst. 2004; 5:203–208. [PubMed: 15803439]
35. Sampaio WO, Nascimento AA, Santos RA. Systemic and regional hemodynamic effects of angiotensin-(1–7) in rats. Am J Physiol Heart Circ Physiol. 2003; 284:H1985–H1994. [PubMed: 12573992]
36. AbdAlla S, Lother H, Abdel-tawab AM, Quitterer U. The angiotensin II AT2 receptor is an AT1 receptor antagonist. J Biol Chem. 2001; 276:39721–39726. [PubMed: 11507095]
37. Rehman A, Leibowitz A, Yamamoto N, Rautureau Y, Paradis P, Schiffrin EL. Angiotensin type 2 receptor agonist compound 21 reduces vascular injury and myocardial fibrosis in stroke-prone spontaneously hypertensive rats. Hypertension. 2011; 59:291–299. [PubMed: 22184324]
38. Kaschina E, Grzesiak A, Li J, Foryst-Ludwig A, Timm M, Rompe F, Sommerfeld M, Kemnitz UR, Curato C, Namsolleck P, et al. Angiotensin II type 2 receptor stimulation: a novel option of therapeutic interference with the renin-angiotensin system in myocardial infarction? Circulation. 2008; 118:2523–2532. [PubMed: 19029468]
39. Lauer D, Slavic S, Sommerfeld M, Thone-Reineke C, Sharkovska Y, Hallberg A, Dahlof B, Kintscher U, Unger T, Steckelings UM, et al. Angiotensin type 2 receptor stimulation ameliorates left ventricular fibrosis and dysfunction via regulation of tissue inhibitor of matrix metalloproteinase 1/matrix metalloproteinase 9 axis and transforming growth factor beta1 in the rat heart. Hypertension. 2014; 63:e60–e67. [PubMed: 24379181]
40. Sriramula S, Cardinale JP, Lazartigues E, Francis J. ACE2 overexpression in the paraventricular nucleus attenuates angiotensin II-induced hypertension. Cardiovasc Res. 2011; 92:401–408. [PubMed: 21952934]
41. Zhu L, Carretero OA, Xu J, Harding P, Ramadurai N, Gu X, Peterson EL, Yang XP. Activation of angiotensin II type 2 receptor suppresses TNF-α-induced ICAM-1 via NF-κB: possible role of ACE2. Am J Physiol Heart Circ Physiol. 2015 ajpheart.00814.2014.

42. Ali Q, Wu Y, Hussain T. Chronic AT2 receptor activation increases renal ACE2 activity, attenuates AT1 receptor function and blood pressure in obese Zucker rats. Kidney Int. 2013; 84:931–939. [PubMed: 23823602]

43. Castro CH, Santos RA, Ferreira AJ, Bader M, Alenina N, Almeida AP. Evidence for a functional interaction of the angiotensin-(1–7) receptor Mas with AT1 and AT2 receptors in the mouse heart. Hypertension. 2005; 46:937–942. [PubMed: 16157793]

44. Bruce E, Shenoy V, Rathinasabapathy A, Espejo A, Horowitz A, Oswalt A, Francis J, Nair A, Unger T, Raizada MK, et al. Selective activation of angiotensin AT2 receptors attenuates progression of pulmonary hypertension and inhibits cardiopulmonary fibrosis. Br J Pharmacol. 2015; 172:2219–2231. [PubMed: 25522140]

45. Chamsi-Pasha MA, Shao Z, Tang WH. Angiotensin-converting enzyme 2 as a therapeutic target for heart failure. Curr Heart Fail Rep. 2014; 11:58–63. [PubMed: 24293035]

46. Wang WK, Wang B, Lu QH, Zhang W, Qin WD, Liu XJ, Liu XQ, An FS, Zhang Y, Zhang MX. Inhibition of high-mobility group box 1 improves myocardial fibrosis and dysfunction in diabetic cardiomyopathy. Int J Cardiol. 2014; 172:202–212. [PubMed: 24485636]

Key messages

- ACE2 knock-in animals have a normal phenotype.
- Overexpression of ACE2 favorably shifts the balance of the RAS to vasoprotective axis.
- Overexpression of ACE2 represses ischemia-induced elevation of HMGB1 and inflammatory cytokines.

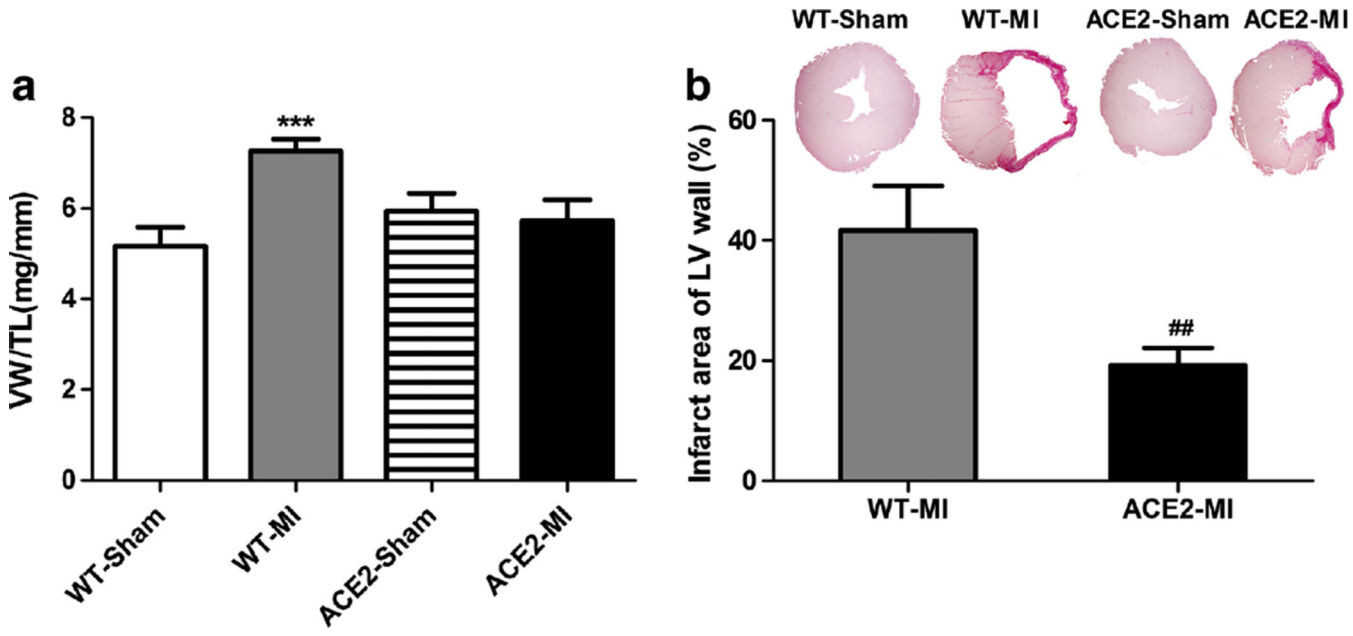

Fig. 1.

Overexpression of ACE2 prevents the myocardial infarction (MI)-induced left ventricle cardiac remodeling. **a** Ventricular hypertrophy reflected by ventricular weight to tibia length ratio (VW/TL). **b** Infarct size was reflected by percentage of the infarcted area to the cross-section of left ventricle free wall. Values are means±SE, n=8–10/group; $^{***}p<0.01$ WT-MI vs. WT-Sham and ACE2-MI; $^{\#\#}p<0.01$ ACE2-MI vs. WT-Sham

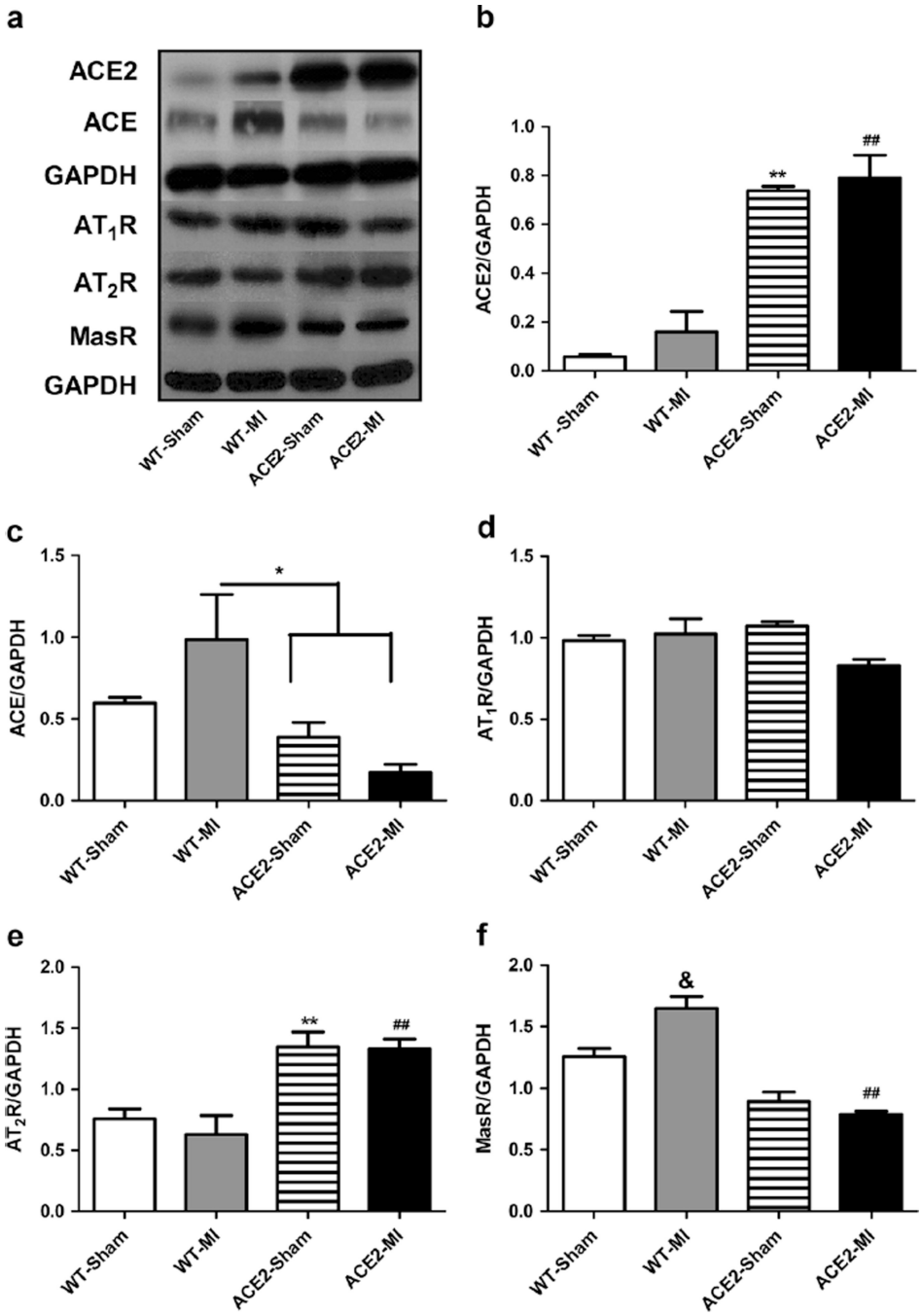

Fig. 2.

Overexpression of ACE2 and ischemia modulate expression of components of renin-angiotensin system in the myocardium of WT and ACE2 animals. **a** Representative western blots showing protein levels of ACE2, ACE, AT_1R, AT_2R, and Mas R and corresponding densitometric analysis (**b–f**). Values are means±SE, n=4–5/group; $^{**}p<0.01$ ACE2-Sham vs. WT-Sham and WT-MI; $^{\#\#}p<0.01$ ACE2-MI vs. WT-Sham and WT-MI; $^{*}p<0.05$ WT-MI vs. ACE2-Sham and ACE2-MI; &$p<0.05$ WT-MI vs. all other groups; $^{+}p<0.05$ ACE2-Sham vs. WT-Sham

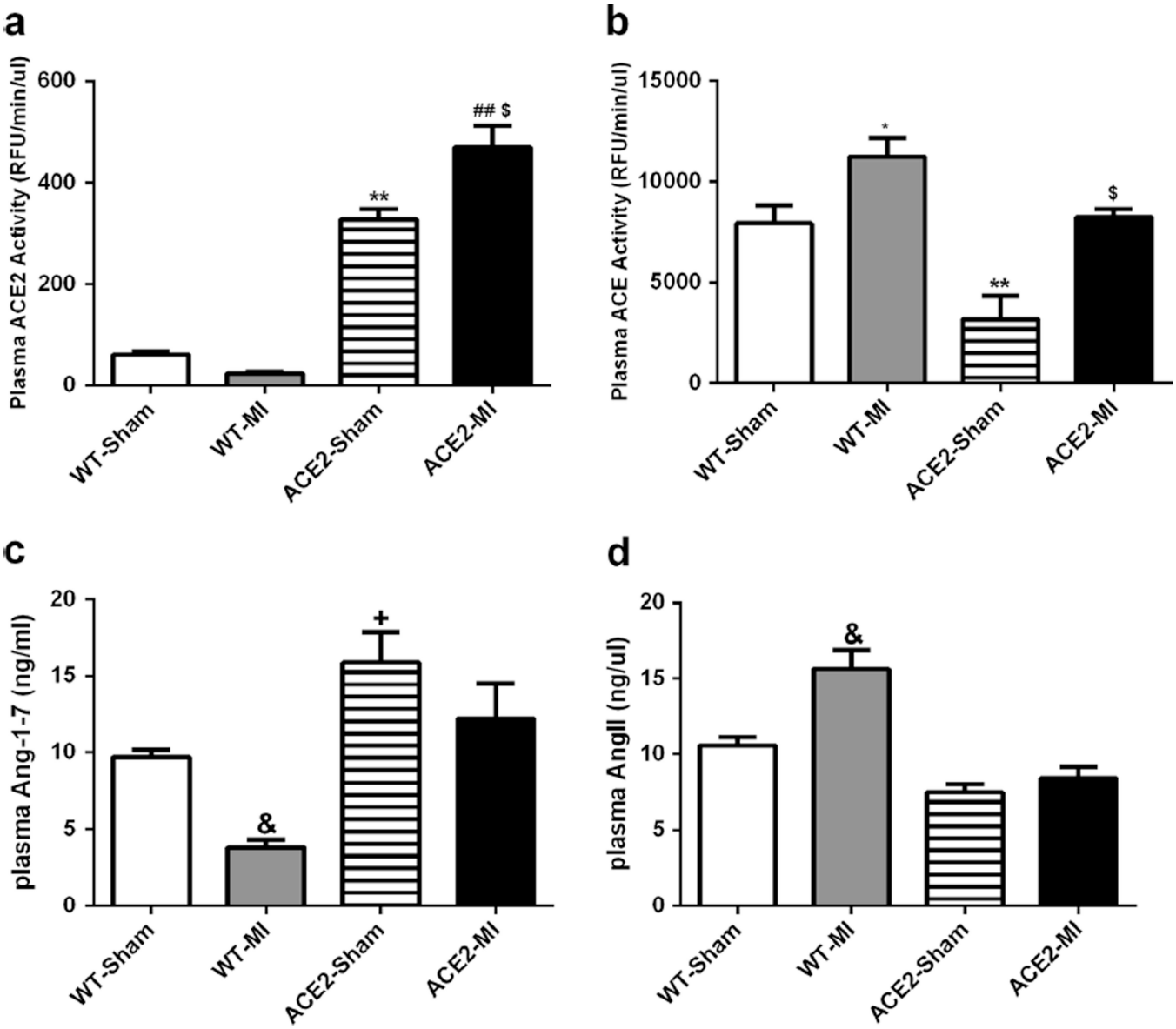

Fig. 3.

Overexpression of ACE2 and ischemia alter plasma ACE2 and ACE activities (**a–b**), and Ang-(1–7) and AngII levels (**c–d**). Values are means±SE, n=8–10/group; &p<0.05 WT-MI vs. all other groups; $^{**}p$<0.01 ACE2-Sham vs. WT-Sham and WT-MI; $^{\#\#}p$<0.01 ACE2-MI vs. WT-Sham and WT-MI; $^{\$}p$<0.05 ACE2-MI vs. ACE2-Sham; $^{*}p$<0.05 WT-MI vs. ACE2-Sham and ACE2-MI

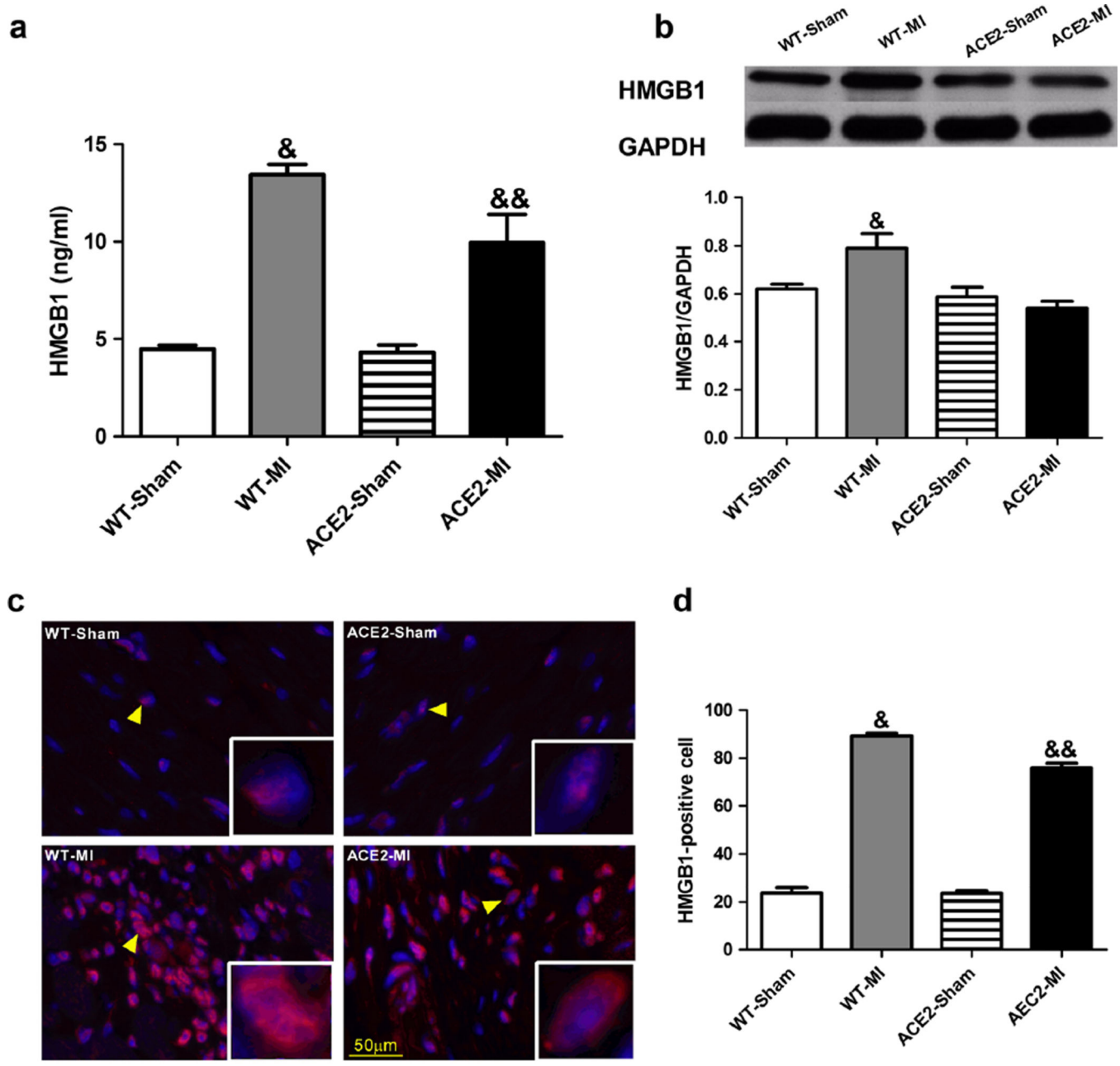

Fig. 4.

Overexpression of ACE2 and ischemia modifies levels of HMGB1 in the plasma and myocardium. **a** Plasma levels of HMGB1 was quantified using ELISA kit. **b** Representative western blot and densitometric analysis for the tissue levels of HMGB1. **c** Representative immunofluorescence images of HMGB1 in the peri-infarct area. Nuclei were stained with DAPI (4′,6-diamidino-2-phenylindol; blue fluorescence). HMGB1 is found in the nuclei in sham animals whereas it is present in both nuclei and cytoplasm (red fluorescence, indicated by *yellow arrows*). HMGB1-positive cells (red fluorescence) were counted using ImageJ and normalized to the total nuclei (**d**). Values are means±SE, n=4–5/group; &p<0.05 WT-MI vs.

all other groups; &&p<0.05 ACE2-MI vs. WT-Sham and ACE2-Sham; $^{\$}p$<0.05 ACE2-MI vs. ACE2-Sham

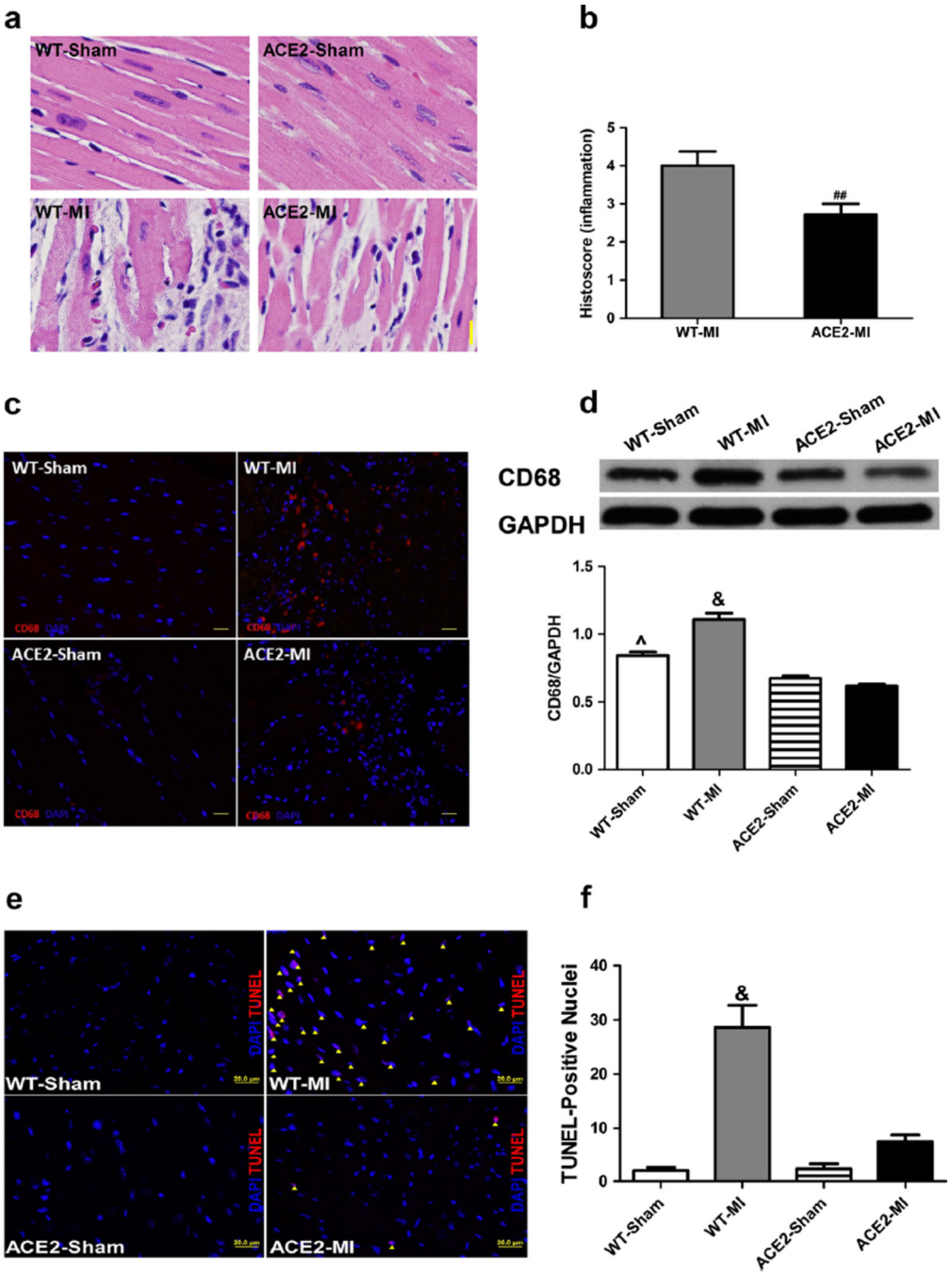

Fig. 5.

Overexpression of ACE2 inhibits infiltration of inflammatory cells including CD68 in the ischemic myocardium and reduces the cardiac damage. **a** Representative images of cardiac HE staining and **b** the average histopathological scores. **c** Representative immunofluorescence images of CD68 in the peri-infarct area. Nuclei were stained with DAPI and CD68-positive cells were stained in red fluorescence. **d** Representative western blot and densitometric analysis for the tissue levels of CD68. Representative TUNEL-staining images (**e**) and quantification of apoptosis (**f**). TUNEL-positive cells (apoptotic

cells, *purple color*) were stained in red, merged with DAPI-stained nuclei (*blue*), and counted as the number of TUNEL-positive cells, which were indicated by a *yellow arrow head*. Values are means±SE, n=4–5/group; &p<0.05 WT-MI vs. all other groups; $^{\wedge}p$<0.05 WT-Sham vs. ACE2-Sham and ACE2-MI; $^{\#\#}p$<0.05 vs. WT-MI

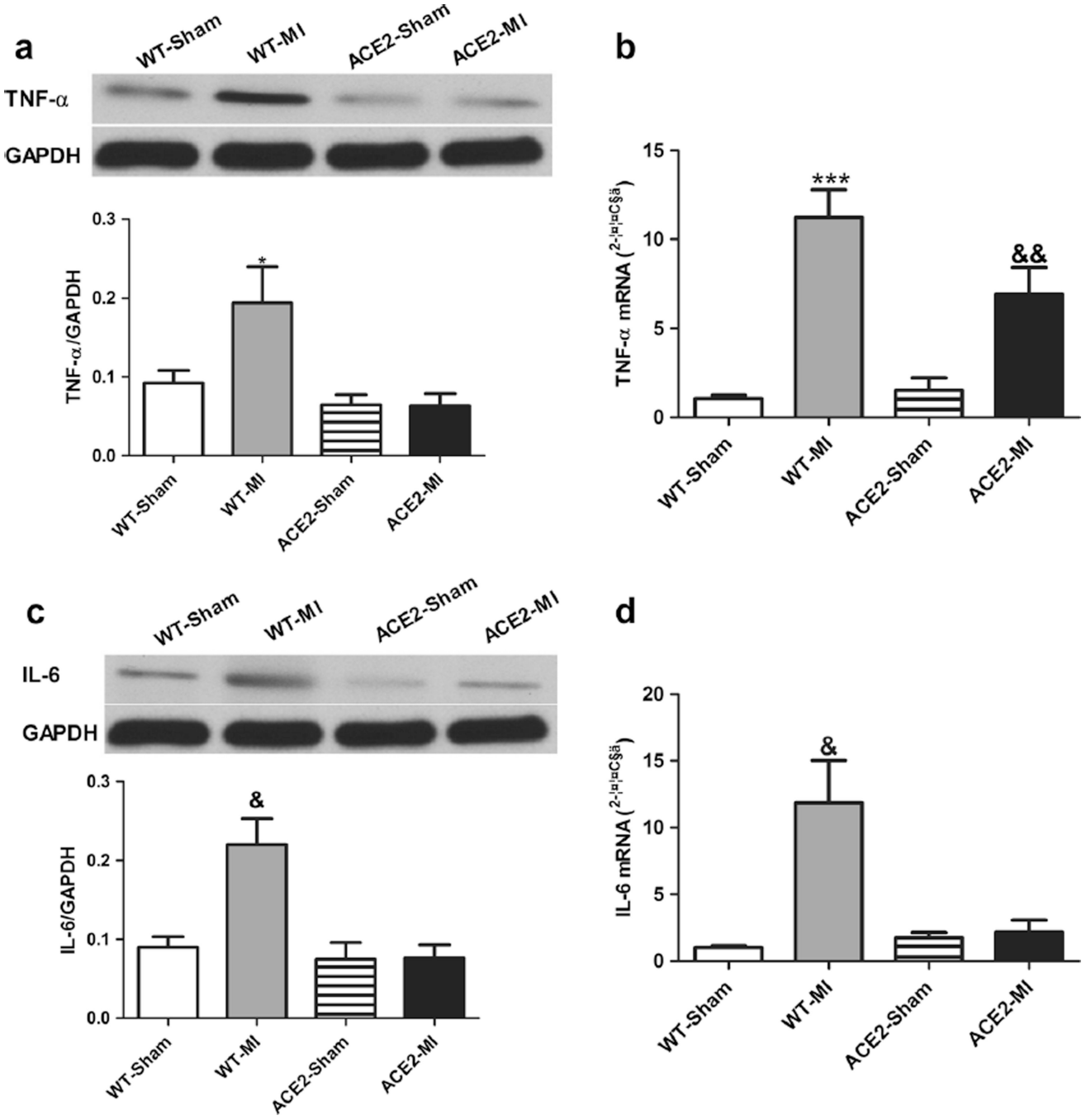

Fig. 6.

Overexpression of ACE2 attenuates inflammatory following MI. Representative western blots and corresponding densitometric analysis and mRNA levels of TNF-α (**a, b**) and IL-6 (**c, d**). Values are means±SE, n=4–6/group; $^{*}p<0.05$ WT-MI vs. ACE2-Sham and ACE2-MI;&$p<0.05$ WT-MI vs. all other groups; $^{***}p<0.01$ WT-MI vs. WT-Sham and ACE2-MI; &&$p<0.05$ ACE2-MI vs. WT-Sham and ACE2-Sham

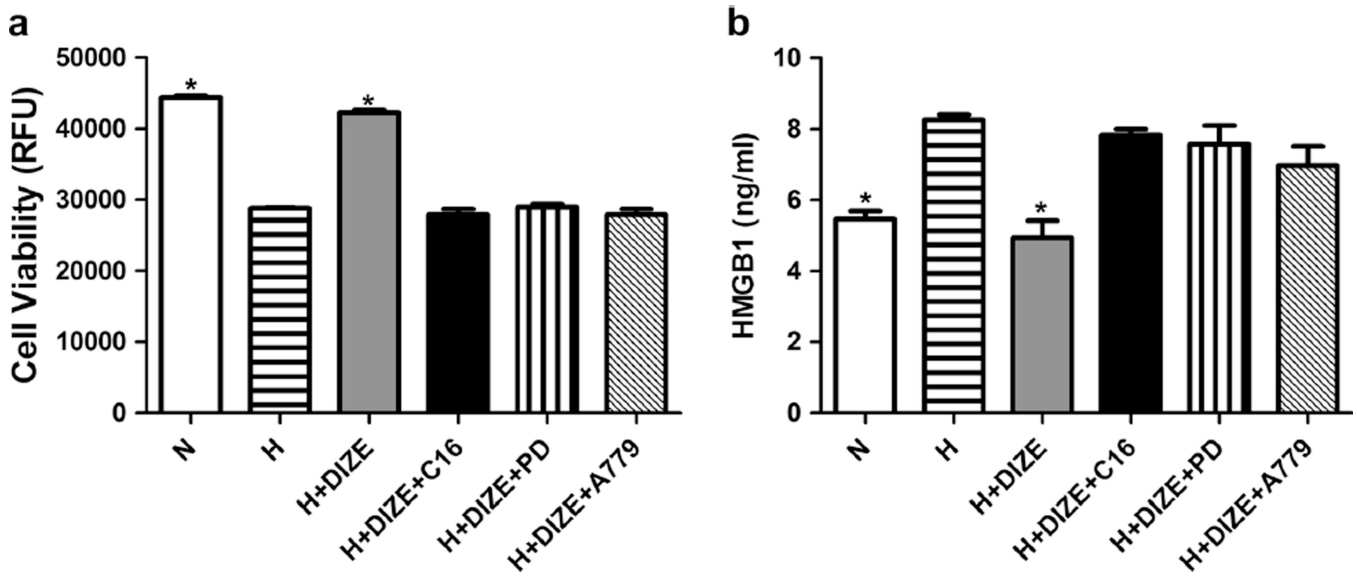

Fig. 7.

Diminazene aceturate (DIZE) treatment protects adult rabbit cardiac myocytes against hypoxia (H)-induced cell death and elevation of HMGB1, which are blocked by selective ACE2, AT2R, and Mas R antagonists. **a** Cells were treated with normoxic condition, H, H +DIZE, H+DIZE+C16, H+DIZE+PD, and H+DIZE+A779 1 h before initiation of hypoxic condition and 4 h for hypoxia. Cell viability was positively correlated with the fluorescence intensity. **b** HMGB1 in the culture medium was collected after 4 h of hypoxic treatment and analyzed using ELISA kit. Each *bar* represents three independent experiments. $n=3$. $^{*}p<0.05$, N and H+DIZE vs. all other groups

Table 1

ACE2 and ACE gene expression in vital organs of WT and ACE2 mice

Organs	WT mice			ACE2 mice		
	ACE2	ACE	ACE2/ACE	ACE2	ACE	ACE2/ACE
Heart	1.11±0.22	1.07±0.28	1.08±0.19	64.04±2.79**	1.10±0.29	98.18±13.62**
Brain (PVN)	1.05±0.17	1.04±0.15	1.05±0.15	230.66±45.39**	1.87±0.21*	124.33±25.39**
Lung	1.05±0.16	1.05±0.17	1.15±0.29	16.77±5.84*	0.81±0.15	21.26±6.73*
Liver	2.10±1.05	1.05±0.12	1.96±0.95	282.02±64.35**	1.09±0.25	249.04±6.22**
Kidney	1.19±0.35	1.10±0.10	1.13±0.30	5.67±0.74**	0.94±0.24	6.80±1.55**
Spleen	1.35±0.46	1.04±0.19	1.17±0.26	67.33±20.65**	1.30±0.32	49.21±5.48**

PVN indicates the paraventricular nucleus. Each value represents mean±SE (n=8–10)

* p<0.05 vs. WT mice;

** p<0.01 vs. WT mice

Table 2

Cardiac hemodynamics of WT and ACE2 KI mice following MI

Cardiovascular function	WT-Sham	WT-MI	ACE2-Sham	ACE2-MI
EF (%)	72.56±3.26	29.05±2.81**	65.70±3.05	51.59±3.37†
ESV (ml)	0.04±0.01	0.28±0.04**	0.06±0.01	0.13±0.02††
EDV (ml)	0.14±0.01	0.39±0.04**	0.16±0.01	0.26±0.04†
LVEDP (mmHg)	6.56±0.68	9.96±1.19*	4.23±0.17	5.59±0.74†
dP/dt_{max} (mmHg/s)	9119.8±470.2	3696.5±324.5**	7869.0±1456.5	5153.1±418.1†#
dP/dt_{min} (mmHg/s)	−6918.2±209.2	−2701.7±320.7**	−6130.0±875.7	−4187.4±306.5†#
MAP (mmHg)	83.84±1.89	73.48±2.41	71.02±3.58	76.65±4.99
HR (bpm)	483.7±7.9	431.6±18.1	484.0±17.6	436.4±14.6

Echocardiographic results and hemodynamic parameters: *EF* ejection fraction, *ESV* end-systolic volume, *EDV* end-diastolic volume, *LVEDP* left ventricle end-diastolic pressure, *MAP* mean arterial pressure, *HR* heart rate. Each value represents mean±SE (n=8–10);

* p<0.05 vs. WT-Sham;

** p<0.01 vs. WT-Sham;

† p<0.05 vs. WT-MI;

†† p<0.01 vs. WT-MI;

# p<0.05 vs. ACE2-Sham